Hardy's Test and CHSH Test of Local Realism

Najeeb Ullah
Roll no: 2022-12-0007
Email: 22120007@lums.edu.pk
LUMS School of Science and Engineering

Monday, April 24, 2023

1 Abstract

We perform two experiments that show a violation of *any* local hidden variable theory (HVT) but in accord with quantum mechanics hence corroborating the concepts of entanglement, non-locality, and non-reality: a system not having a definite state prior to a measurement. We use polarization entangled photon pairs, produced in type-I SPDC, to perform Hardy's test and the CHSH test. For Hardy' test, we get $H = 0.0196 \pm 0.0006$ which violates the inequality $H \leq 0$ (predicted by an HVT) by 34 standard deviations. Similarly, for the CHSH test, we get $S = 2.33 \pm 0.03$ which violates the inequality $|S| \leq 2$ (predicted by an HVT) by 11 standard deviations.

2 Introduction

Locality means that an independent measurement of the state of a particle cannot alter the measurement outcome of the state of another particle. Reality means that a particle has a definite state regardless of measurement. These two concepts appear particularly intuitive that we may regard them as axioms of our universe. And if any theory makes predictions contrary to any of these *assumptions* must be wrong, or at best incomplete! This was the argument of Einstein, Podolsky, and Rosen in their famous paper on entanglement and the Copenhagen interpretation of quantum mechanics. Quantum mechanics predicts that these assumptions can be violated under some circumstances involving entangled systems; Entanglement is when the state of a multi-particle system cannot be written as a direct product of the single-particle states. This means that we cannot define the state of a single particle in such system hence running counter to the reality assumption. Furthermore, a measurement of the state of a single particle collapses the states of *all* other particles in the system to definite values hence running counter to the locality assumption.

This conflict between quantum mechanics and any theory based on local realism remained a 'philosophical' debate for many decades until John Bell showed that it can be tested: he derived an inequality that must be obeyed by *any* theory based on local realism, and that quantum mechanics predicts a violation of these inequalities. Now it was the experimentalists job to design an experiment to prove who was right: Einstein or quantum mechanics.

However, Bell's original inequality was for ideal systems so other researchers derived inequalities for non-ideal systems: these are collectively called Bell's inequalities.

The first such inequality and the experiment testing it was presented and done by Freedman. For optical systems (using entangled photons), the inequality due to Clauser, Horne, Shimony, and Holt (CHSH) is employed which is conceptually harder to comprehend. Yet another Bell's inequality was derived by Hardy and experiments based on it has also been performed. The results of all these experiments unanimously confirm the predictions of quantum mechanics.

We perform Hardy's test and the CHSH test and use as our system photon pairs produced in a process called type-I spontaneous parametric downconversion.

3 Generating Entangled Photons [1]

As mentioned above, any test of local realism involves entangled particles. An accessible way of generating entangled particles is using a process called type-I spontaneous parametric downconversion (SPDC) that produces a photon pair with their polarizations entangled. We employ this process.

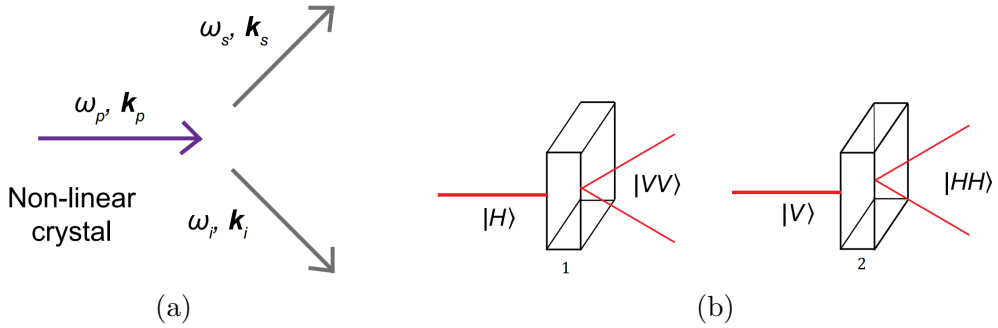

Figure 1: (a) Schematic of SPDC and (b) schematic of type-I SPDC.

In SPDC, a photon incident on a birefringent crystal (such as a beta-Barium Borate crystal) is absorbed and subsequently two photons are emitted in compliance *only* with the laws of conservation of energy and momentum (Figure 1a). But we can cut the crystal such that the polarizations of the photons in the pair are the same and orthogonal to the incident photon's polarization: this is called type-I SPDC (Figure 1b). We can further choose the material and geometry of our crystal such that the downconverted pair has half the frequency and twice the wavelength of

the incident photon and the pair emerge from the crystal at 3° to the incident photon's propagation direction [1].

To produce a polarization-entangled pair of photons, we use two such crystals and align their optical axes orthogonally (Figure 2): this allows the downconversion of horizontally polarized photons in one of the crystals and vertically polarized photons in the other crystal (with the assumption that these stacked crystals are placed perfectly horizontal and straight up). An incident photon with both horizontal and vertical components becomes

$$\sqrt{A}|V\rangle + \sqrt{1-A}|H\rangle \longrightarrow \sqrt{A}|HH\rangle + \sqrt{1-A}e^{i\phi}|VV\rangle \tag{1}$$

(without loss of generality, we have assumed a zero phase difference in the initial state as it can be absorbed in the phase difference introduced by the BBO crystals). We can control the parameter, A, by inserting a half-wave plate before the BBO crystals. A quartz crystal (also a birefringent material) can be inserted before the BBO crystals to control ϕ. This way, we can create any bipartite-entangled state we require.

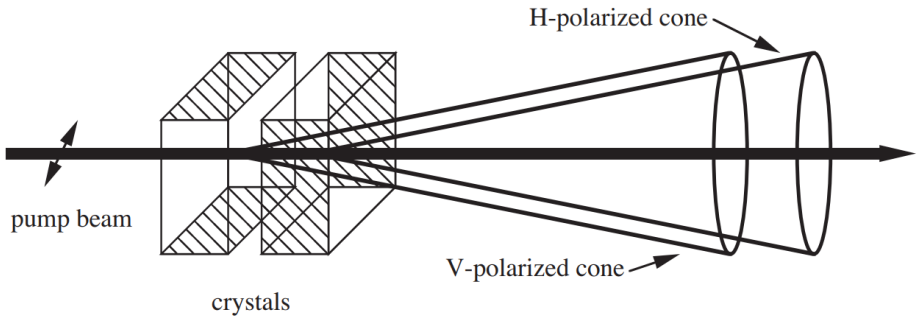

Figure 2: The crystals are each 0.5 mm thick and in contact face-to-face. The pump beam is $\sim$ 1 mm in diameter so the downconverted cones overlap almost completely. For a pump beam containing both horizontally and vertically polarized photons, an entangled state is generated.

4 Experimental Setup

The final apparatus is shown in Figure 3 which will be used in both Hardy's test and the CHSH test. However, setting it up requires multiple intermediate steps each requiring accurate placement of the different components shown. We delineate these steps below.

[1]The outgoing photon beams will actually form a cone because of the Uncertainty principle: the uncertainty in the position of this pair when it's produced is finite so the uncertainty in their momentum must also be finite and nonzero. This is why the coincidence counts are significantly less than the single counts ($\sim$ 10%).

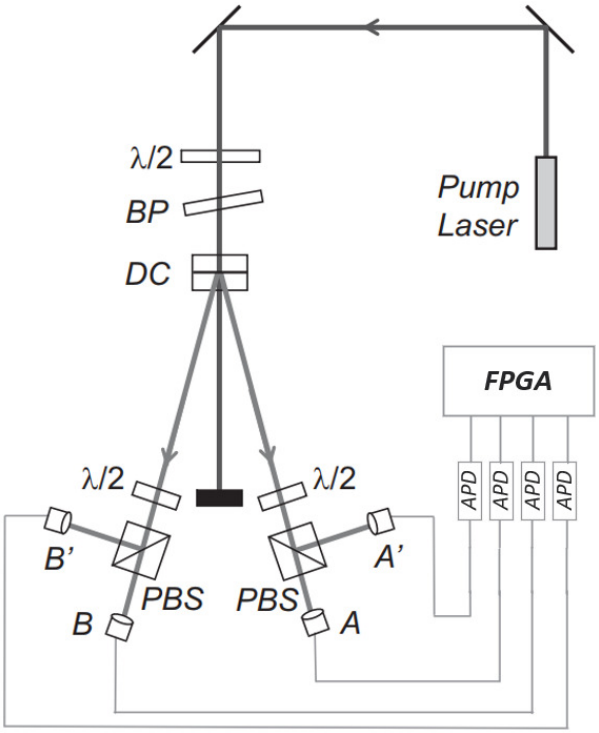

Figure 3: Here $\lambda 2/$ is a half-wave plate, BP a birefringent plate, DC the downconversion crystals, PBS a polarizing beam splitter, APD the avalanche photo-diode, and FPGA the field-programmable gate array.

4.1 Aligning the Crystals

We collectively refer to a set of collection optics (collimators and fiber optics) and a photodetector as a 'detector'.

1. The 405 nm pump laser should be mounted so that its polarization is vertical (or horizontal) and it must be collimated: our laser is vertically polarized and collimated.

2. Using two mirrors, the pump beam can be aligned so that it travels level to the optical table or breadboard at a consistent height (and better yet, along the holes on the breadboard), as shown in Figure 4.

3. Make sure that the **detectors are turned off**.

4. Insert the 405 nm HWP and the BBO crystals in the path of the pump beam and set the HWP's fast axis to vertical.

5. Since the downconverted photon beams make an angle of $\pm 3^\circ$ with reference to the pump beam, detector A is placed facing the downconversion crystal, roughly at $\pm 3^\circ$ with respect to the pump beam.

6. Detector A is coarsely aligned using the alignment laser by making it fall onto the center of the BBO stack.

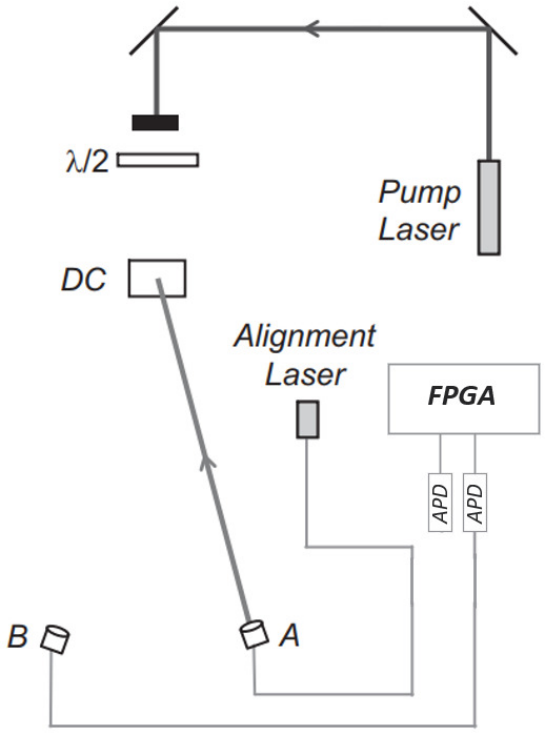

Figure 4: Using the alignment laser the beam should travel backward from the collection optics, and onto the center of the downconversion crystals. This coarsely aligns detector A and the crystals: detector B is coarsely aligned in a similar fashion.

7. The alignment laser is removed and detector A is connected with the respective APD (avalanche photo-diode).

8. Insert a beam block in front of the BBO crystals to block the unconverted photon beam.

9. Start the accompanying software (`photo-detection.py`) for recording the detection counts.

10. Turn off the lights and turn on the LED's above the breadboard.

11. Turn on the APD: the knobs of the detector A mount are adjusted to optimize its vertical and horizontal tilts so that the detected count rate is maximized. We slightly slide the detector A mount sideways to optimize the beam detection angle.

12. Using the adjustment screws on the crystal mount, slowly tilt the crystal horizontally, while monitoring the counts on detector-A. If the count rate is sensitive to this tilt, adjust the tilt to maximize the count rate. If the count rate is insensitive to this tilt, then use the other knob to tilt it vertically. Again, try to maximize the count rate on detector A.

13. Now set the pump HWP at 45° to make the pump beam horizontal: this means that now the other crystal will be responsible for its downconversion.

14. Using the adjustment screws on the crystal mount, slowly tilt the crystal vertically (or horizontally, depending on what was observed in the previous step), while trying to maximize the counts on detector-A.

This aligns the crystals reasonably well. After completing the full alignment of both detectors (as described below) we want to once again carefully adjust the tilt of the crystal in order to maximize the coincidence count rate.

4.2 Aligning Detectors A and B

1. Place detector B roughly facing the BBO crystals and making an angle of 3° with the pump beam as shown in Figure 4.

2. Coarse alignment of detectors A and B is obtained as described above.

3. Remove the alignment laser and connect the SPCMs (detectors+FPGA) with detectors A and B.

4. Fine tuning of detector A is done by maximizing the single counts on A when the pump beam is turned on.

5. Fine tuning of detector B is done by maximizing the coincidence counts AB.

A reasonably high coincidence counts (around 10% of the single counts) substantiates accurate alignment of the components.

4.3 Aligning the Beam Splitters and Detectors A′ and B′

1. Insert the polarizing beam splitter (PBS) a few inches away from detector B as in Figure 5.

2. Roughly place detector B′ at the reflection side of the PBS and equidistant from it as detector B is.

3. Connect one alignment laser with detector B and one with detector B′.

4. Collimate these beams on the PBS and then position the PBS to make these fall on its center. Adjusting the position of detector B′ should make the two alignment beams fall exactly at the center of the PBS.

5. Now collimate these beams onto the BBO crystals.

6. Make them fall on the center of the BBO stack by adjusting the PBS mount knobs.

7. Fine tuning of the PBS and detector B′ is done by maximizing the AB′ coincidence counts.

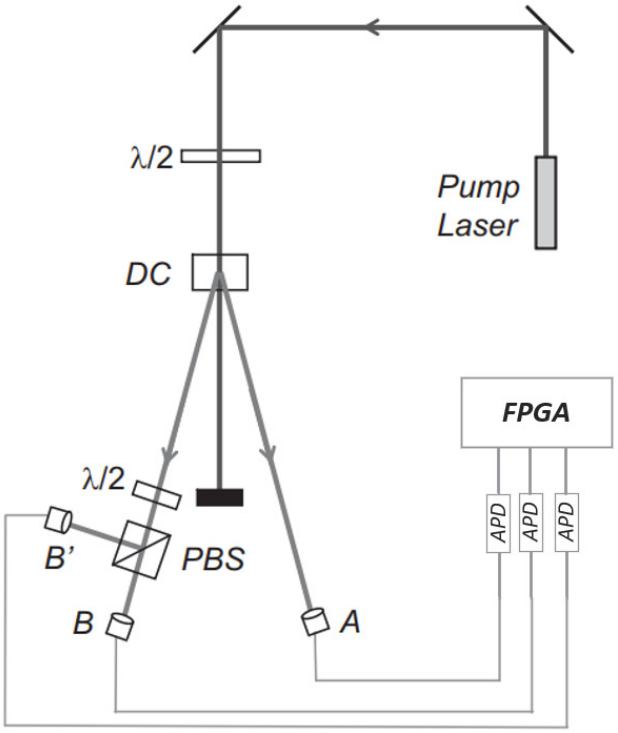

Figure 5: Aligning the PBS and the detector B′: the PBS in the other beam and the detector A′ is aligned in similar fashion.

8. A PBS in front of detector A and the detector A′ are inserted and aligned in a similar fashion.

This completes our setup as shown in Figure 3.

5 Creating a Specific Entangled State

As mentioned before, we can use the pump HWP and the quartz crystal to create any specific entangled state we want. The logic behind this and the procedure is presented here.

5.1 Wavefunction for the CHSH Test

We start with the wavefunction required for the CHSH test which is easier to comprehend and make. The general state produced by the BBO crystals is

$$|\psi\rangle = \sqrt{A}|HH\rangle + \sqrt{1-A}e^{i\phi}|VV\rangle \tag{2}$$

and the CHSH test requires the below maximally entangled state

$$|\psi\rangle = \frac{1}{\sqrt{2}}\left(|HH\rangle + |VV\rangle\right) \tag{3}$$

We obtain (3) from (2) by proceeding as follows:

1. Set the HWPs in the signal and the idler beams at 0° allowing us to make measurements in the HV-basis (see Appendix B).

2. The A and B detectors measure $|V\rangle$ and the A′ and B′ detectors measure $|H\rangle$. Hence the ratio of the AB and A′B′ coincidence counts sets the ratio of $|VV\rangle$ and $|HH\rangle$ in (2).

3. Making these coincidence counts equal makes $A = 1/2$ in (2).

4. Now we rotate both the HWPs to 22.5° allowing us to make measurements in the DA-basis (see Appendix B).

5. We now minimize either A′B or AB′. This achieves the state (3).

The state from the source is now

$$|\psi\rangle = \frac{1}{\sqrt{2}}\left(|HH\rangle + e^{i\phi}|VV\rangle\right) \tag{4}$$

The HWPs convert this into

$$|\psi\rangle = \frac{1}{\sqrt{2}}\left(|DD\rangle + e^{i\phi}|AA\rangle\right) \tag{5}$$

where $|D\rangle$ is the diagonal state and $|A\rangle$ is the anti-diagonal state. The probability of an A′B coincidence becomes

$$P_{A'B} = |\langle HV|\psi\rangle|^2 \tag{6}$$

$$\langle HV|\psi\rangle = \frac{1}{\sqrt{2}}\left[\langle HV|DD\rangle + e^{i\phi}\langle HV|AA\rangle\right] \tag{7}$$

$$= \frac{1}{\sqrt{2}}\left[\frac{1}{\sqrt{2}}\frac{1}{\sqrt{2}} + e^{i\phi}\frac{1}{\sqrt{2}}\left(-\frac{1}{\sqrt{2}}\right)\right] \tag{8}$$

For this to be 0, we must have $\phi = 0$. Hence minimizing A′B (or equivalently AB′) renders $\phi = 0$.

5.2 Wavefunction for Hardy's Test

Hardy's test requires the below state

$$|\psi\rangle = \sqrt{0.2}|HH\rangle + \sqrt{0.8}|VV\rangle \tag{9}$$

We obtain (9) from (2) by proceeding as follows:

1. As described above, setting the ratio of the AB and A′B′ coincidence counts sets the ratio of $|VV\rangle$ and $|HH\rangle$ in (2). We now set these coincidence counts in 4 : 1 ratio which makes $A = 0.2$ in (2) making it

$$|\psi\rangle = \sqrt{0.2}|HH\rangle + \sqrt{0.8}e^{i\phi}|VV\rangle \tag{10}$$

2. To set $\phi = 0$ in the above equation, we minimize $P(-\alpha, \alpha)$: set the HWPs in the signal and the idler channels to $-\alpha/2$ and $\alpha/2$ and minimize the A′B′ coincidence counts (see Appendix B).

The joint probability of detecting the signal and the idler photons to be polarized along θ_A and θ_B, respectively, is (Appendix E)

$$\begin{aligned} P(\theta_A, \theta_B) &= |\langle \theta_A \theta_B | \psi \rangle|^2 && (11) \\ \langle \theta_A \theta_B | \psi \rangle &= \sqrt{0.2} \langle \theta_A \theta_B | HH \rangle + \sqrt{0.8} e^{i\phi} \langle \theta_A \theta_B | VV \rangle && (12) \\ &= \sqrt{0.2} \cos\theta_A \cos\theta_B + \sqrt{0.8} e^{i\phi} \sin\theta_A \sin\theta_B && (13) \end{aligned}$$

Let $\theta_A = -\theta$ and $\theta_B = \theta$ (we can also assume the signs to be reversed; all that matters is that they must have opposite signs). Then (24) becomes

$$\langle -\theta\theta | \psi \rangle = \sqrt{0.2} \cos^2\theta - \sqrt{0.8} e^{i\phi} \sin^2\theta \quad (14)$$

Assume $\phi = 0$, then we have

$$\langle -\theta\theta | \psi \rangle = \sqrt{0.2} \cos^2\theta - \sqrt{0.8} \sin^2\theta \quad (15)$$

This has solutions $\theta \approx \pm 35^\circ$ and $\pm 145^\circ$: The $\pm 145^\circ$ directions are identical to the $\mp 35^\circ$ directions, respectively, and as we have mentioned above, the sign of θ does not matter so we pick $\theta = 35^\circ$. For this value of θ, (22) becomes

$$P(-\alpha, \alpha) \approx 0.3 - 0.3 e^{i\phi} \quad (16)$$

This is why minimizing $P(-\alpha, \alpha)$ renders $\phi = 0$ for the Hardy state, (9).

6 Hardy's Test of Local Realism [1]

Let $P(\theta_A, \theta_B)$ represent the joint probability that the signal photon is polarized along θ_A and the idler photon is polarized along θ_B. Then it can be shown that for *any* local realistic theory we must have

$$P(\theta_{A1}, \theta_{B1}) \leq P(\theta_{A2}, \theta_{B2}) + P(\theta_{A1}, \theta_{B2}^{\perp}) + P(\theta_{A2}^{\perp}, \theta_{B1}) \quad (17)$$

for *any* θ_{A1}, θ_{B1}, θ_{A2}, and θ_{B2}. This is called the Bell-Clauser-Horne inequality. Choosing $\theta_{A1} = \beta$, $\theta_{B1} = -\beta$, $\theta_{A2} = -\alpha$, and $\theta_{B2} = \alpha$, it can be rearranged as

$$0 \geq P(\beta, -\beta) - P(\beta, \alpha^{\perp}) - P(-\alpha^{\perp}, -\beta) - P(-\alpha, \alpha) \quad (18)$$

and defining

$$H = P(\beta, -\beta) - P(\beta, \alpha^{\perp}) - P(-\alpha^{\perp}, -\beta) - P(-\alpha, \alpha) \quad (19)$$

means

$$H \leq 0 \quad (20)$$

for *any* theory based on local realism. However, the quantum mechanical expression for the joint probability, $P(\theta_{Ai}, \theta_{Bj})$, for a bipartite system in the general state

$$|\psi\rangle = \sqrt{A}\,|HH\rangle + \sqrt{1-A}\,|VV\rangle \tag{21}$$

is given by

$$\begin{aligned} P(\theta_{Ai}, \theta_{Bj}) &= |\langle\theta_{Ai}\theta_{Bj}|\psi\rangle|^2 && (22)\\ &= \left(\sqrt{A}\langle\theta_{Ai}\theta_{Bj}|HH\rangle + \sqrt{1-A}\langle\theta_{Ai}\theta_{Bj}|VV\rangle\right)^2 && (23)\\ &= \left(\sqrt{A}\cos\theta_{Ai}\cos\theta_{Bj} + \sqrt{1-A}\sin\theta_{Ai}\sin\theta_{Bj}\right)^2 && (24) \end{aligned}$$

Using this expression in (19) we can show (see Appendix C) that the maximal violation of (20) is attained by these states and analyses angles:

$$\begin{aligned} |\Psi_1\rangle &= \sqrt{0.8}|HH\rangle + \sqrt{0.2}|VV\rangle, \qquad \alpha = 55^\circ \text{ and } \beta = 71^\circ && (25)\\ |\Psi_2\rangle &= \sqrt{0.2}|HH\rangle + \sqrt{0.8}|VV\rangle, \qquad \alpha = 35^\circ \text{ and } \beta = 19^\circ && (26) \end{aligned}$$

6.1 Experiment and the result

After setting up the apparatus (Figure 3) as described in section (4), we wish to find H from (19) for the state (26). We can create this state by following the procedure in section 5.2.

To find H, we need to find the four joint probabilities in (19) for $\alpha = 35^\circ$ and $\beta = 19^\circ$. Since we are using a HWP+PBS as an effective polarizer we need to set the HWPs at *half* the angles with respect to the horizontal and track the counts of the *horizontal* channels of the PBSs, which are A′ and B′ (see Appendix B). This means that the joint probability, $P(\theta_A, \theta_B)$, in terms of the coincidence counts, is

$$P(\theta_A, \theta_B) = \frac{N_{A'B'}}{N_{AB} + N_{A'B} + N_{AB'} + N_{A'B'}} \tag{27}$$

The coincidence counts are taken for an integration time of 120 s and the probabilities turn out to be

$$\begin{aligned} P(\beta, -\beta) &= 0.1161 \pm 0.0004 && (28)\\ P(\beta, \alpha^\perp) &= 0.0356 \pm 0.0002 && (29)\\ P(-\alpha^\perp, -\beta) &= 0.0235 \pm 0.0002 && (30)\\ P(-\alpha, \alpha) &= 0.0375 \pm 0.0002 && (31) \end{aligned}$$

and hence we get

$$H = 0.0196 \pm 0.0006 \tag{32}$$

This violates $H \leq 0$ by 34 standard deviations! A conclusive violation of local realism.

7 CHSH Test of Local Realism [1]

Let $P(\alpha, \beta)$ represent the joint probability that the signal photon is polarized along α and the idler photon is polarized along β. In the previous section, we did not derive an expression for this using local realism, and instead came up with an inequality involving these joint probabilities that must be true regardless of their actual expressions (although, we did derive its quantum mechanical expression). Clauser, Horne, Shimony, and Holt derived such an expression for these joint probabilities based on local realism and they are:

$$P(\alpha,\beta) = \int \left(\frac{1-A(\alpha,\lambda)}{2}\right)\left(\frac{1-B(\beta,\lambda)}{2}\right) p(\lambda)d\lambda \tag{33}$$

$$P(\alpha^{\perp},\beta) = \int \left(\frac{1+A(\alpha,\lambda)}{2}\right)\left(\frac{1-B(\beta,\lambda)}{2}\right) p(\lambda)d\lambda \tag{34}$$

$$P(\alpha,\beta^{\perp}) = \int \left(\frac{1-A(\alpha,\lambda)}{2}\right)\left(\frac{1+B(\beta,\lambda)}{2}\right) p(\lambda)d\lambda \tag{35}$$

$$P(\alpha^{\perp},\beta^{\perp}) = \int \left(\frac{1+A(\alpha,\lambda)}{2}\right)\left(\frac{1+B(\beta,\lambda)}{2}\right) p(\lambda)d\lambda \tag{36}$$

where $p(\lambda)$ is the hidden variable's normalized probability distribution, $A(\alpha, \lambda)$ is a function that determines the measurement outcome of the idler photon, and $B(\beta, \lambda)$ is a function that determines the measurement outcome of the signal photon. These functions incorporate the local realism hypothesis: the state of each photon is determined by the hidden variable, λ, (reality) and the measurement outcome of one of them cannot affect the measurement outcome of the other since A is not a function of β and B is not a function of α (locality). $A(\alpha, \lambda)$ takes the value of -1 when the idler photon is polarized along α and the value of $+1$ when it is polarized along $\alpha^{\perp}$; similar explanation holds for $B(\beta, \lambda)$.

We can make intuitive sense of these integrals. Take the integral for $P(\alpha^{\perp}, \beta^{\perp})$ for instance: for a specific λ, the factor corresponding to the idler photon, $(1 + A(\alpha, \lambda))/2$, will be either 0 or 1 depending on whether it is polarized along α or $\alpha^{\perp}$, respectively. Similarly, the factor corresponding to the signal photon, $(1 + B(\beta, \lambda))/2$, will be either 0 or 1 depending on whether it is polarized along β or $\beta^{\perp}$, respectively. Hence, these terms will only contribute to the overall probability when both the photons are polarized along $\alpha^{\perp}$ and $\beta^{\perp}$.

Additionally, they showed that the expected outcome of a measurement of the idler photon to be polarized along α and the signal photon to be polarized along β is

$$E(\alpha,\beta) \equiv P(\alpha,\beta) + P(\alpha^{\perp},\beta^{\perp}) - P(\alpha,\beta^{\perp}) - P(\alpha^{\perp},\beta) \tag{37}$$

and according to local realism, using (33)−(36), it must be

$$E(\alpha,\beta) = \int A(\alpha,\lambda)B(\beta,\lambda)p(\lambda)d\lambda \tag{38}$$

We now define a quantity whose physical significance or interpretation is not obvious, but its utility will become clear in a moment:

$$s = A(a,\lambda)(B(b,\lambda) - B(b',\lambda)) + A(a',\lambda)(B(b,\lambda) + B(b',\lambda)) \tag{39}$$

Since each instance of $A(\theta,\lambda)$ and $B(\theta,\lambda)$ can take the values of either -1 or 1 we can see that s can take the values of either -2 or 2. Its average is found using (38):

$$S \equiv \langle s \rangle = \int s(\lambda, a, a', b, b') p(\lambda) d\lambda \tag{40}$$

$$= E(a,b) - E(a,b') + E(a',b) + E(a',b') \tag{41}$$

Since s can only be ± 2, S must satisfy

$$|S| \leq 2 \tag{42}$$

This must be true if local realism is true.

However, as derived in section 6, the quantum mechanical expression for the joint probability, $P(\alpha,\beta)$, is

$$P(\alpha,\beta) = \left(\sqrt{A}\cos\alpha\cos\beta + \sqrt{1-A}\sin\alpha\sin\beta\right)^2 \tag{43}$$

for the state

$$|\psi\rangle = \sqrt{A}|HH\rangle + \sqrt{1-A}|VV\rangle \tag{44}$$

The CHSH test requires $A = 1/2$ so

$$|\psi\rangle = \frac{1}{\sqrt{2}}(|HH\rangle + |VV\rangle) \tag{45}$$

$$P(\alpha,\beta) = \frac{1}{2}(\cos\alpha\cos\beta + \sin\alpha\sin\beta)^2 \tag{46}$$

Using (46) to evaluate (37) we get

$$E(a,b) = \frac{1}{2}\cos^2(a-b) + \frac{1}{2}\cos^2(a-b) - \frac{1}{2}\sin^2(a-b) - \frac{1}{2}\sin^2(a-b) \tag{47}$$

$$E(a,b) = \cos(2(a-b)) \tag{48}$$

and S from (41) becomes

$$S = \cos(2(a-b)) - \cos(2(a-b')) + \cos(2(a'-b)) + \cos(2(a'-b')) \tag{49}$$

As discussed in Appendix D, we get the maximum value of $S = 2\sqrt{2}$ for any $0 \leq a \leq 180°$, $a' = a + 45°$, $b = a + 22.5°$, and $b' = a + 67.5°$.

This means that for the entangled state, (45), and the analyses angles defined above, we must obtain $S > 2$ which will prove a violation of local realism.

7.1 Experiment and the result

After setting up the apparatus (Figure 3) as described in section (4), we wish to find S from (49) for the state (45). We can create this state by following the procedure in section 5.1.

We choose $a = -45^\circ$ so the other angles become: $a' = 0^\circ$, $b = -22.5^\circ$, and $b' = 22.5^\circ$. Since we are using a HWP+PBS as an effective polarizer we need to set the HWPs at *half* the angles with respect to the horizontal and track the counts of the *horizontal* channels of the PBSs, which are A′ and B′ (see Appendix B). This means that the joint probability, $P(\theta_A, \theta_B)$, in terms of the coincidence counts, is

$$P(\theta_A, \theta_B) = \frac{N_{A'B'}}{N_{AB} + N_{A'B} + N_{AB'} + N_{A'B'}} \tag{50}$$

For each term in (41) we have to find four joint probabilities as given in (37). The coincidence counts are taken for an integration time of 30 s and we get

$$S = 2.33 \pm 0.03 \tag{51}$$

This violates $|S| \leq 2$ by 11 standard deviations! A conclusive violation of local realism.

8 Conclusions

Using technologies available in an undergraduate laboratory we have created a single-photon source which can be used to demonstrate the following:

1. We can prove the existence of photons (since the photoelectric effect is actually not a proof of their existence) and hence show the particle nature of light.
2. We can then show the interference of these single photons hence proving their wave nature.
3. We can obtain violations of Bell's inequalities and hence disprove local realism and any hidden variable theory. This also proves
   - that entanglement is possible and real,
   - the Copenhagen interpretation of quantum mechanics,
   - and the concept of wave collapse of a particle upon measurement.

After configuring the experimental setup, performing these tests are surprisingly simple yet they probe some of the deepest aspects of physical reality. This provides the students an access to higher-level physics.

Appendix A Creating a Single-Photon Source

We have implicitly assumed from the beginning that the photons created in the downconversion process constitutes a single-photon source, i.e., we have only *one* photon pair present in our apparatus at a time. Let us now justify this.

Our laser is operating at a power of 50 mW and has a wavelength of 405 nm which means the average number of photons hitting the BBO stack is $\sim 10^{17}$ per second. The efficiency of downconversion is $\sim 10^{-10}$ so we have $\sim 10^7$ downconverted pairs headed towards our detectors per second. The inefficiency of our detectors (collimators+SPCMs) and the non-perfect alignment results in only $\sim 10^5$ single counts per second. Additionally, due to the fact that the photons in a downconverted pair travel in a cone the coincidence counts is still smaller at ~ 8000 per second.

These photon pairs can either arrive at the detectors uniformly across the one second span or be grouped together and strike the detectors within our coincidence window of ~ 20 ns (partial grouping is also similar). We have to verify that these are not grouped (a.k.a. bunched together): we do this experimentally.

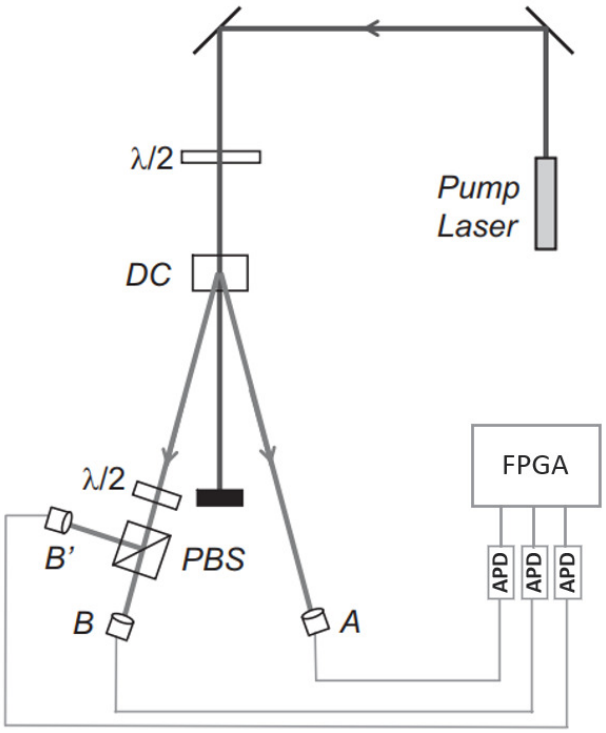

Figure 6: Experimental setup to verify our single-photon source.

We place a PBS in the signal arm in front of the detectors B and B′ and a HWP before this PBS (Figure 6). This HWP is set at 22.5° in order to make the signal beam diagonally polarized. Any single photon arriving at the PBS will then either be reflected or transmitted with equal probabilities. This means that we must get an N_{AB} or an $N_{AB'}$ coincidence count at a time but not an $N_{ABB'}$ triple coincidence count. Now imagine our photons pairs to be bunched together which will mean that multiple photons will strike the PBS within our coincidence window and hence with equal probabilities be reflected and transmitted: since they are temporally separated by less than 20 ns and are being reflected and transmitted we must get significant triple coincidence counts, $N_{ABB'}$. But experimentally, we get only 1 or 2 (at most 3) triple coincidence counts which are actually accidental triple coincidence counts (when three uncorrelated photons hit the detectors within the coincidence window). This proves that the temporal separation between the photon

pairs is at least greater than the coincidence window. Because of the enormous speed at which photons travel a temporal separation of at least 20 ns means a spatial separation of at least 6 m. Given that the length of our whole apparatus is ~ 1 m we can be certain that we have only one photon pair present in our setup at a time.

Appendix B HWP + PBS ≡ Polarizer

We can use the combination of a polarizing beam splitter and a half wave plate as a polarizer. Let an incoming light of polarization $\vec{\mathbf{E}}$ making an angle α with the horizontal be incident on a polarizer oriented at angle θ with the horizontal as shown in Figure (7a): The component $|\vec{\mathbf{E}}|\cos(\alpha-\theta)$ will be transmitted and the other component $\vec{\mathbf{E}}\sin(\alpha-\theta)$ will be absorbed. A half wave plate rotates an incident $\vec{\mathbf{E}}$ by 180° about its fast axis which is equivalent to reflecting the $\vec{\mathbf{E}}$ about the fast axis such that the angle between them remains the same, Figure (7b). If we set the HWP at $\theta/2$ with the horizontal then the angle between the incident $\vec{\mathbf{E}}$ and the HWP will be $\alpha-\theta/2$ which will also be the angle between the final $\vec{\mathbf{E}}$ and the HWP: This makes the final $\vec{\mathbf{E}}$'s angle with the horizontal to be $(\alpha-\theta/2)-\theta/2 = \alpha-\theta$. Placing a polarizing beam splitter in the path of this rotated $\vec{\mathbf{E}}$ will split its horizontal component, $|\vec{\mathbf{E}}|\cos(\alpha-\theta)$, and its vertical component, $|\vec{\mathbf{E}}|\sin(\alpha-\theta)$. Hence the horizontal output channel of the PBS will give us the same component of the incident $\vec{\mathbf{E}}$ as a polarizer would with the added advantage that, unlike a polarizer, it doesn't absorb the vertical component.
Note that the *vectors* emerging from the polarizer and the HWP are different since the former makes an angle of θ with the horizontal and the latter makes an angle of 0° with the horizontal: but their *magnitudes* are the same, $|\vec{\mathbf{E}}|\cos(\alpha-\theta)$.

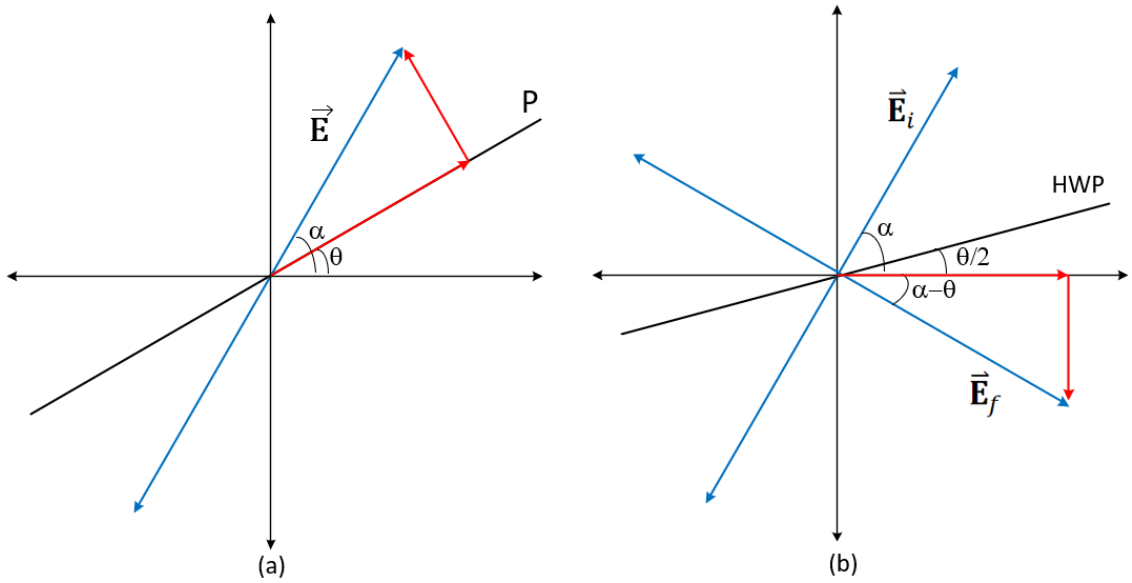

Figure 7: (a) Schematic of how a polarizer polarizes an incident light, and (b) how a half wave plate plus a polarizing beam splitter effectively accomplishes the same outcome.

This can be verified with Jones calculus. The Jones matrices of a polarizer and a HWP, and the Jones vector of an incident $\vec{\mathbf{E}}$ are:

$$\mathbf{J}_P(\theta) = \begin{pmatrix} \cos^2\theta & \sin\theta\cos\theta \\ \sin\theta\cos\theta & \sin^2\theta \end{pmatrix}, \mathbf{J}_{HWP}(\theta) = \begin{pmatrix} \cos 2\theta & \sin 2\theta \\ \sin 2\theta & -\cos 2\theta \end{pmatrix} \tag{52}$$

$$\mathsf{e} = E \begin{pmatrix} \cos\alpha \\ \sin\alpha \end{pmatrix} \tag{53}$$

The field after a polarizer becomes:

$$\mathbf{J}_P(\theta)\mathsf{e} = E \begin{pmatrix} \cos^2\theta & \sin\theta\cos\theta \\ \sin\theta\cos\theta & \sin^2\theta \end{pmatrix} \begin{pmatrix} \cos\alpha \\ \sin\alpha \end{pmatrix} = E \begin{pmatrix} \cos(\theta)\cos(\alpha-\theta) \\ \sin(\theta)\cos(\alpha-\theta) \end{pmatrix} \tag{54}$$

The field after a HWP at $\theta/2$ becomes:

$$\mathbf{J}_{HWP}(\theta)\mathsf{e} = E \begin{pmatrix} \cos\theta & \sin\theta \\ \sin\theta & -\cos\theta \end{pmatrix} \begin{pmatrix} \cos\alpha \\ \sin\alpha \end{pmatrix} = E \begin{pmatrix} \cos(\alpha-\theta) \\ -\sin(\alpha-\theta) \end{pmatrix} \tag{55}$$

The magnitude of (54) is $|E\cos(\alpha-\theta)|$ and the magnitude of the horizontal component of (55) is also $|E\cos(\alpha-\theta)|$.

Appendix C Hardy's Test: Wavefunctions and Analyses Angles

For an entangled state of the down-converted pair of photons

$$|\psi\rangle = \sqrt{A}\,|HH\rangle + \sqrt{1-A}\,|VV\rangle \tag{56}$$

quantum mechanics gives the joint probability of the signal photon to be polarized along θ_A and the idler photon to be polarized along θ_B to be

$$P(\theta_A,\theta_B) = \left(\sqrt{A}\cos\theta_A\cos\theta_B + \sqrt{1-A}\sin\theta_A\sin\theta_B\right)^2 \tag{57}$$

and a local realistic theory predicts

$$P(\beta,\alpha^\perp) + P(-\alpha^\perp,-\beta) + P(-\alpha,\alpha) \;\geq\; P(\beta,-\beta) \tag{58}$$

for *any* choice of α (and $\alpha^\perp = \alpha + 90$), β, and the state $|\psi\rangle$ which amounts to choosing A in (75). If we *choose* α, β, and A such that

$$P(\beta,\alpha^\perp) = 0 \tag{59}$$

$$P(-\alpha^\perp,-\beta) = 0 \tag{60}$$

$$P(-\alpha,\alpha) = 0 \tag{61}$$

then (58) predicts:

$$P(\beta,-\beta) \leq 0 \tag{62}$$

$$P(\beta,-\beta) = 0 \tag{63}$$

since probabilities cannot be negative. We will now derive, using (57), multiple sets of values of α, β, and A which satisfy (59)-(61) but not (63) hence violating local realism. Evaluating (59)-(61) using (57) we get

$$P(\beta, \alpha^{\perp}) = \left(\sqrt{A}\,\cos\beta\sin\alpha - \sqrt{1-A}\,\cos\alpha\sin\beta\right)^2 = 0 \tag{64}$$

$$P(-\alpha^{\perp}, -\beta) = \left(\sqrt{A}\,\cos\beta\sin\alpha - \sqrt{1-A}\,\cos\alpha\sin\beta\right)^2 = 0 \tag{65}$$

$$P(-\alpha, \alpha) = \left(\sqrt{A}\,\cos^2\alpha - \sqrt{1-A}\,\sin^2\alpha\right)^2 = 0 \tag{66}$$

We note that (64) and (65) are identical so we proceed with (64) and (66) and get:

$$\tan^2\alpha = \sqrt{\frac{A}{1-A}} \tag{67}$$

$$\tan\beta = \left(\frac{A}{1-A}\right)^{3/4} \tag{68}$$

and (68) gives

$$\tan^2\beta = \left(\frac{A}{1-A}\right)^{3/2} \Longrightarrow \sec^2\beta = 1 + \left(\frac{A}{1-A}\right)^{3/2} \tag{69}$$

$$\cos^2\beta = \left[1 + \left(\frac{A}{1-A}\right)^{3/2}\right]^{-1} \tag{70}$$

similarly, we get

$$\tan^2\beta = \left(\frac{A}{1-A}\right)^{3/2} \Longrightarrow \sin^2\beta = \left(\frac{A}{1-A}\right)^{3/2}\cos^2\beta \tag{71}$$

$$\sin^2\beta = \left(\frac{A}{1-A}\right)^{3/2}\left[1 + \left(\frac{A}{1-A}\right)^{3/2}\right]^{-1} \tag{72}$$

Hence $P(\beta, -\beta)$ becomes

$$P(\beta, -\beta) = \left(\sqrt{A}\cos^2\beta - \sqrt{1-A}\sin^2\beta\right)^2 \tag{73}$$

$$P(A) = A\,(1-2A)^2\left(1 + A\left(\sqrt{\frac{A}{1-A}} - 1\right)\right)^{-2} \tag{74}$$

A plot of this function in Figure 8 reveals that there are multiple states for the same value of $P(\beta, -\beta)$. We can find its maximum and the corresponding α and β using equations (67) and (68) respectively, giving us the values in Table 1.

We choose to pick a simple value of A, 0.2 and 0.8, and find the corresponding analyses angles and the probabilities, Table 2. Note that the constraints in (59)-(61) makes $H = P(\beta, -\beta)$.

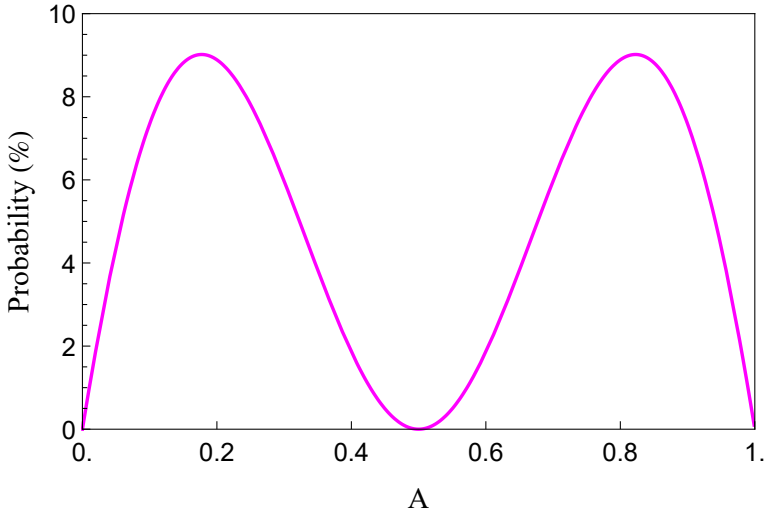

Figure 8: $P(\beta, -\beta)$ as a function of degree of entanglement A.

$P(\beta,-\beta)$	0.0901699	0.0901699
A	0.17735	0.82265
α	72.4434°	55.7293°
β	17.556°	34.2707°

Table 1: Maximum value of $P(\beta, -\beta)$ and the corresponding wavefunction specification, A, and the analyses angles, α and β.

$P(\beta,-\beta)$	0.0888889	0.0888889
A	0.2	0.8
α	35.2644°	54.7356°
β	19.4712°	70.5288°

Table 2: Convenient choice of wavefunction and the corresponding analyses angles.

Appendix D CHSH Test: Wavefunction and Analysis Angles

CHSH test requires a maximally entangled state such as

$$|\psi\rangle = \frac{1}{\sqrt{2}}\left(|HH\rangle + |VV\rangle\right) \tag{75}$$

We define a quantity S given by

$$S = E(a,b) - E(a,b') + E(a',b) + E(a',b') \tag{76}$$

where

$$E(a,b) = P_{VV}(a,b) + P_{HH}(a,b) - P_{HV}(a,b) - P_{VH}(a,b) \tag{77}$$

whose physical significance or interpretation is not obvious but it can be shown to obey

$$|S| \leq 2 \tag{78}$$

for *any* hidden variable theory and *any* set of arbitrary polarizer angles, a, a', b, and b'. However, quantum mechanics predicts

$$S \leq 2\sqrt{2} \tag{79}$$

which means that for some choices of a, a', b, and b' we can get

$$2 < S \leq 2\sqrt{2} \tag{80}$$

and hence disprove *all* hidden variable theories.
The reason for this is because a hidden variable theory and quantum mechanics give *different* expressions for the joint probability, $P_{ij}(a,b)$ for $i,j = \{H,V\}$. Tsirelson showed [2, 3] that the upper bound of S is $2\sqrt{2}$ and this constrains the angles to be $a' = a + 45^\circ$ and $b' = b + 45^\circ$ making S a function of a and b only:

$$S = 2\left[\cos(2(a-b)) - \sin(2(a-b))\right] \tag{81}$$

Solving $S = 2\sqrt{2}$ gives

$$b = a + \frac{1}{2}\left(\frac{\pi}{4} - 2\pi n\right), \qquad n \in \mathbb{Z} \tag{82}$$

All values of n give the same value of b upto a multiple of 2π so we take $n = 0$ which yields $b = a + \pi/8$. This makes $S = 2\sqrt{2}$ for *any* $0 \leq a \leq \pi$.

Appendix E Uncertainty Calculations

- Each detector receives photons even when the pump laser is turned off; these are called background counts. Since these are not due to downconversion we simply subtract them from the single counts of each detector.
- Each pair of detectors has accidental coincidence counts which are due to two photons, not part of the same pair produced in the downconversion process, hitting the detectors within their coincidence window ($\Delta t \sim 20$ ns). These are given by $N_{AB} \approx N_A N_B \Delta t$. Similar expressions hold for other pairs of the detectors. These also need to be subtracted from the coincidence counts given by the SPCMs.
- The uncertainty in each coincidence count is simply the standard uncertainty in the mean: since we get coincidence counts for each second of our integration time.
- Then the propagated uncertainty in the probabilities is

$$\sigma P_{AB} = P_{AB}\sqrt{\left(\frac{\sigma N_{AB}}{N_{AB}}\right)^2 + \left(\frac{\sqrt{(\sigma N_{AB})^2 + (\sigma N_{A'B})^2 + (\sigma N_{AB'})^2 + (\sigma N_{A'B'})^2}}{N_{AB} + N_{A'B} + N_{AB'} + N_{A'B'}}\right)^2} \tag{83}$$

  with similar expressions for the other probabilities.
- Finally, the uncertainties in H, E, and S are given by

$$\sigma H = \sqrt{(\sigma P_{\beta,-\beta})^2 + (\sigma P_{\beta,\alpha^\perp})^2 + (\sigma P_{-\alpha^\perp,-\beta})^2 + (\sigma P_{-\alpha,\alpha})^2} \tag{84}$$

$$\sigma E = \sqrt{(\sigma P_{\alpha,\beta})^2 + (\sigma P_{\alpha^\perp,\beta^\perp})^2 + (\sigma P_{\alpha,\beta^\perp})^2 + (\sigma P_{\alpha^\perp,\beta})^2} \tag{85}$$

$$\sigma S = \sqrt{(\sigma E_{a,b})^2 + (\sigma E_{a,b'})^2 + (\sigma E_{a',b})^2 + (\sigma E_{a',b'})^2} \tag{86}$$

- Lastly, the confidence intervals are calculated as

$$\frac{|H_{expected} - H_{experimental}|}{\sigma H} \qquad \text{and} \qquad \frac{|S_{expected} - S_{experimental}|}{\sigma S} \tag{87}$$

References

[1] M. Waseem, Faizan-e-Ilahi, and M. Anwar, "*Quantum Mechanics in the Single Photon Laboratory*", Lahore University of Management Sciences, (2020 edition), ch. 4-5.

[2] https : //en.wikipedia.org/wiki/CHSH_inequality

[3] R. Brewster, G. Baumgartner, and Y. Chembo, "*Quantum analysis of polarization entanglement degradation induced by multiple-photon pair generation*, 11 Aug, 2021, doi: 10.1103/PhysRevA.104.022411